Eur. Phys. J. B **32**, 291–296 (2003)
DOI: 10.1140/epjb/e2003-00100-1

THE EUROPEAN PHYSICAL JOURNAL B

Extended nature of coupled optical interface modes in Thue-Morse dielectric superlattices

Sheng-Feng Cheng and Guo-Jun Jin[a]

National Laboratory of Solid State Microstructures and Department of Physics, Nanjing University, Nanjing 210093, PR China

Received 24 September 2002 / Received in final form 11 January 2003
Published online 11 April 2003 –

Abstract. We investigate coupled optical interface modes in Thue-Morse (TM) dielectric superlattices composed of two kinds of materials with frequency-dependent dielectric functions. Four basic transfer matrices are derived in the dielectric continuum approximation. By a standard matrix operation method, the trace map of the global transfer matrix in this configuration is obtained. Under Born-von Kármán boundary conditions, the frequency spectra are calculated and their branching rules together with the *quartet* property are elucidated. It is further proved rigorously that nearly all eigenmodes in this framework have *extended* nature. The quartet of the eigenmodes is illuminated analytically. The common features and pronounced differences compared with coupled optical interface modes in periodic and Fibonacci dielectric superlattices as well as with other collective elementary excitations in TM structures are also revealed.

PACS. 63.20.Dj Phonon states and bands, normal modes, and phonon dispersion – 68.35.Ja Surface and interface dynamics and vibrations – 71.45.-d Collective effects 61.44.Br Quasicrystals

1 Introduction

The discovery of quasicrystal by Shechtman *et al.* in 1984 has inspired much interest concerning the physical properties of the so-called quasiperiodic structures [1]. As a representative one-dimensional model of a quasicrystal, the Fibonacci lattice has gained a great deal of attention and becomes a hotly investigated subject. Many new advances, along with some earlier results about the incommensurate discrete Schrödinger equation, provide us with an approach to understand the crossover from periodicity to disorder. Subsequently, other aperiodic but yet deterministic structures come to the attention of researchers. One example is the Thue-Morse (TM) lattice. The speciality of this structure is that it has no translational invariance but supports delocalized electronic states [2,3], which implies that it is an intermedium linking perfect periodic and Fibonacci structures. Because of this point, the TM sequence has attracted much attention in recent years [4]. Until now we have known that the energy spectrum of electrons in a TM chain, which is calculated in the on-site model, is similar to a Cantor set [2], and under certain circumstances the Fourier transform of a TM chain is singular continuous [5]. Moreover, the electronic and vibrational properties of a TM lattice in a general model have also been studied [6,7].

On the other hand, from the standpoints of experimenters, the significant progress in the fabrication technology can supply us with many elaborate artificial structures. Thus a feasible way to explore the physical behavior in aperiodic systems is to construct semiconductor, metal, or dielectric superlattices according to corresponding aperiodic sequences. To understand the results of experiments, it is useful to study the elementary excitations in these aperiodic structures, as an natural expansion of the excitations in periodic superlattices [8,9]. Among many kinds of excitations in superlattices, the optical phonons hold an important place and deserve a careful investigation [8], especially in quasiperiodic and aperiodic multilayers [10]. One can see in the following that the optical phonons in a dielectric superlattice usually have two types: the bulklike modes and the interface modes [8]. Interestingly, the latter will be coupled to give collective excitations of the whole structure when the layer thickness of the superlattice is relatively small.

In this paper our main interest is to study the properties of coupled optical interface modes in dielectric superlattices arranged in the TM sequence and to reveal its common features and pronounced differences compared with other elementary excitations in TM structures, such as electrons [3,6,7], acoustic phonons [11], and plasmon polaritons [12]. In Section 2 we first introduce the dielectric continuum approximation for TM superlattices, then the transfer matrices are established and the trace map is derived; in Section 3 we provide calculated results and

[a] e-mail: gjin@nju.edu.cn

theoretical analyses of the frequency spectra and the electrostatic potential distributions, which are the counterparts of the energy spectra and the wave functions of electrons in TM chains; finally a brief summary is presented.

2 Model and formulation

With two building blocks denoted by L and S, we can construct any generation of the TM sequence by the successive substitutions $L \to LS$ and $S \to SL$. If the initial block is chosen as L, this process will give the following sequences $L \to LS \to LSSL \to LSSLSLLS \to LSSLSLLSSLLSLSSL \to \cdots$. On the other hand, if we begin with S, the growing sequences will be $S \to SL \to SLLS \to SLLSLSSL \to SLLSLSSLLSSLSLLS \to \cdots$. To distinguish the neighboring same blocks such as LL and SS, each block of TM superlattices is composed of two layers with different dielectric materials A and B. Thus the jth generation of a TM superlattice has 2^j blocks and 2^{j+1} layers. A and B layers in L and S blocks have the thickness d_L^A, d_L^B, d_S^A, and d_S^B, respectively. Furthermore, A and B layers are with different dielectric functions ε_A and ε_B, which are chosen to be the same as those of the corresponding bulk materials and are frequency dependent by $\varepsilon_{A(B)}(\omega) = \varepsilon_{A(B),\infty}(\omega^2 - \omega^2_{A(B),LO})/(\omega^2 - \omega^2_{A(B),TO})$, where $\omega_{A(B),LO}$ and $\omega_{A(B),TO}$ are frequencies of the longitudinal and transverse optical phonons, and $\varepsilon_{A(B),\infty}$ is the high-frequency limit of the dielectric function.

Here we would like to illustrate the two types of optical phonons in dielectric superlattices, *i.e.*, the bulklike modes and the interface modes. In the long wavelength limit, it is appropriate to adopt the dielectric continuum model, and each optical mode generates a macroscopic electric field $\mathbf{E}$ described by $\nabla \times \mathbf{E} = 0$ and $\nabla \cdot \mathbf{D} = 0$, where $\mathbf{D} = \varepsilon(\omega)\mathbf{E}$. From them we can define an electrostatic potential $\Phi(\mathbf{r}, t)$ to give $\mathbf{E} = -\nabla\Phi(\mathbf{r}, t)$, then in each layer of a superlattice $\Phi(\mathbf{r}, t)$ satisfies the equation $\varepsilon(\omega)\nabla^2\Phi(\mathbf{r}, t) = 0$ [8,13], where $\varepsilon(\omega) = \varepsilon_A(\omega)$ or $\varepsilon_B(\omega)$.

For optical phonons with the frequency $\omega_{A,LO}$, one has $\varepsilon_A(\omega) = 0$, $\varepsilon_B(\omega) \neq 0$, so in A layers $\mathbf{D} = 0$ and in B layers $\nabla^2\Phi(\mathbf{r}, t) = 0$. The boundary conditions at interfaces require that in B layers $\Phi(\mathbf{r}, t) = 0$ and $\mathbf{E} = 0$, *i.e.*, the macroscopic electric fields associated with these modes are confined in A layers. Every layer still holds a sequence of standing-wave resonances identical to those of the bulk dielectric materials A. These modes are bulklike modes. Apparently, the bulklike modes of different dielectric layers do not couple each other. A similar argument can be given for the optical phonons with a frequency $\omega_{B,LO}$, which correspond to the bulklike modes confined in B layers. Furthermore, through Huang's equations [14], one can attest that the optical phonons with frequencies $\omega_{A,TO}$ and $\omega_{B,TO}$ are also bulklike modes.

On the contrary, for the other optical modes, $\varepsilon_A(\omega) \neq 0$ and $\varepsilon_B(\omega) \neq 0$, thus $\nabla^2\Phi(\mathbf{r}, t) = 0$ in the whole superlattice. Through the electrostatic continuum conditions at the interfaces one can find that in this case $\Phi(\mathbf{r}, t)$ attenuates to zero exponentially when one moves away from the interface. The corresponding modes are called interface modes [15]. These modes generate macroscopic electric fields distributing through several adjacent dielectric layers. Therefore, the interface modes locating at neighboring interfaces superpose together, leading to collective excitations of the whole structure, which are capable of transporting energy along the growth direction of the superlattice. Hereafter we call them coupled optical interface modes. Because of the emergence of these coupled modes, the original dispersion relations of bulk dielectric materials are modified and new connections between frequency and wave vector appear. A simple calculation shows frequencies of coupled optical interface modes satisfy $\varepsilon_A(\omega)/\varepsilon_B(\omega) < 0$.

Note that the two surfaces of each superlattice layer are still with periodic lattices and have translational invariance, then the electrostatic potentials associated with the interface modes can be described by a two-dimensional wave vector $\mathbf{k}$ parallel to the interface [8]. Now the $\mathbf{z}$ axis is chosen to be perpendicular to the superlattice planes and denotes the aperiodic direction, and $\mathbf{x}$ is parallel to the superlattice plane. Without loss of generality, we can write the electrostatic potential as $\Phi(\mathbf{r}, t) = \phi(z)\exp[\mathrm{i}(kx - \omega t)]$, where $\mathbf{k}$ is chosen to be along the $\mathbf{x}$ axis, and the nontrivial part $\phi(z)$ satisfies

$$\left(\frac{\mathrm{d}^2}{\mathrm{d}z^2} - k^2\right)\phi(z) = 0. \tag{1}$$

Take n as the layer index and the electrostatic continuum conditions at the interfaces are

$$\phi_n(z) = \phi_{n+1}(z), \quad \varepsilon_n\frac{\mathrm{d}\phi_n(z)}{\mathrm{d}z} = \varepsilon_{n+1}\frac{\mathrm{d}\phi_{n+1}(z)}{\mathrm{d}z}. \tag{2}$$

For the TM superlattice we considered, the solution of equation (1) in the mth block can be written as $\phi_m(z) = p_m\mathrm{e}^{kz} + q_m\mathrm{e}^{-kz}$ in the B layer, and $\phi_m(z) = g_m\mathrm{e}^{kz} + h_m\mathrm{e}^{-kz}$ in the A layer. Thus we have

$$\begin{pmatrix} g_{m+1} \\ h_{m+1} \end{pmatrix} = M_{m+1,m}\begin{pmatrix} g_m \\ h_m \end{pmatrix}, \tag{3}$$

where $M_{m+1,m}$ is a transfer matrix. In the current situation there are only four types of $M_{m+1,m}$'s, which are

$$\begin{aligned}
M_{LL} &= \begin{pmatrix} \alpha_L\mathrm{e}^{kd_L^A} & \beta_L \\ -\beta_L & \gamma_L\mathrm{e}^{-kd_L^A} \end{pmatrix}, \\
M_{SL} &= \begin{pmatrix} \alpha_L\mathrm{e}^{k(d_S^A+d_L^A)/2} & \beta_L\mathrm{e}^{k(d_S^A-d_L^A)/2} \\ -\beta_L\mathrm{e}^{k(d_L^A-d_S^A)/2} & \gamma_L\mathrm{e}^{-k(d_S^A+d_L^A)/2} \end{pmatrix}, \\
M_{LS} &= \begin{pmatrix} \alpha_S\mathrm{e}^{k(d_L^A+d_S^A)/2} & \beta_S\mathrm{e}^{k(d_L^A-d_S^A)/2} \\ -\beta_S\mathrm{e}^{k(d_S^A-d_L^A)/2} & \gamma_S\mathrm{e}^{-k(d_S^A+d_L^A)/2} \end{pmatrix}, \\
M_{SS} &= \begin{pmatrix} \alpha_S\mathrm{e}^{kd_S^A} & \beta_S \\ -\beta_S & \gamma_S\mathrm{e}^{-kd_S^A} \end{pmatrix},
\end{aligned} \tag{4}$$

where

$$\alpha_{L(S)} = \cosh kd^B_{L(S)} + \frac{1}{2}\left(\frac{\varepsilon_B}{\varepsilon_A} + \frac{\varepsilon_A}{\varepsilon_B}\right)\sinh kd^B_{L(S)},$$
$$\beta_{L(S)} = \frac{1}{2}\left(\frac{\varepsilon_B}{\varepsilon_A} - \frac{\varepsilon_A}{\varepsilon_B}\right)\sinh kd^B_{L(S)},$$
$$\gamma_{L(S)} = \cosh kd^B_{L(S)} - \frac{1}{2}\left(\frac{\varepsilon_B}{\varepsilon_A} + \frac{\varepsilon_A}{\varepsilon_B}\right)\sinh kd^B_{L(S)}. \quad (5)$$

The matrices above are all unimodular because $\alpha_{L(S)}\gamma_{L(S)} + \beta^2_{L(S)} = 1$. With these four basic transfer matrices, a rather general model of TM dielectric superlattices is defined. When $d^A_L = d^A_S$ and $d^B_L \neq d^B_S$, it reduces to the common on-site model; on the contrary, if $d^A_L \neq d^A_S$ and $d^B_L = d^B_S$, the conventional transfer model is attained. It is similar to the general models of electrons and classical vibrations in TM chains [6].

By the global equation

$$\begin{pmatrix} g_{N+1} \\ h_{N+1} \end{pmatrix} = M_j \begin{pmatrix} g_1 \\ h_1 \end{pmatrix}, \quad (6)$$

where $N = 2^j$, we can define a global transfer matrix M_j for the jth generation of a TM superlattice. Obviously, M_j is a product of multiplying the four basic matrices M_{LL}, M_{LS}, M_{SL}, and M_{SS} in the proper order. It can also be obtained through the recursion relations

$$M_j = N_{j-1}\overline{N}_{j-1}, \quad \overline{M}_j = \overline{N}_{j-1}N_{j-1},$$
$$N_j = M_{j-1}N_{j-1}, \quad \overline{N}_j = \overline{M}_{j-1}\overline{N}_{j-1}, \quad (7)$$

for $j \geq 1$ and with $M_0 = M_{LL}$, $\overline{M}_0 = M_{SS}$, $N_0 = M_{LS}$, and $\overline{N}_0 = M_{SL}$. For example, the first a few global transfer matrices are $M_1 = M_{LS}M_{SL}$, $M_2 = M_{LL}M_{LS}M_{SS}M_{SL}$, and $M_3 = M_{LS}M_{SL}M_{LL}M_{LS}M_{SL}M_{LS}M_{SS}M_{SL}$, etc.

For matrix iteration, one is always concerned about the trace operation [16]. It can be derived that the global transfer matrices for successive generations of a TM superlattice satisfy a relation, which is

$$M_j = M_{j-2}M_{j-3}M_{j-2}M^{-1}_{j-3}M_{j-1} \quad (j \geq 3), \quad (8)$$

where M^{-1}_{j-3} denotes the converse matrix of M_{j-3}. Defining three traces $r_j = \mathrm{Tr}M_j$, $s_j = \mathrm{Tr}M_{j-1}M^{-1}_{j-2}M_jM_{j-2}$, and $t_j = \mathrm{Tr}M_{j-1}M_j$, one can further obtain

$$r_{j+1} = r_{j-1}s_{j-1}t_{j-1} + r_j - r_{j-2}(s_{j-1} + t_{j-1}),$$
$$s_{j+1} = s_jt_j + r_{j-2}r_{j-1}t_{j-1} - r^2_{j-2} - r^2_{j-1} - t^2_{j-1} + 2,$$
$$t_{j+1} = s_jt_j + r_{j-2}r_{j-1}s_{j-1} - r^2_{j-2} - r^2_{j-1} - s^2_{j-1} + 2, \quad (9)$$

for $j \geq 3$. The trace map above is too intricate. Fortunately, for $j \geq 2$ there is an invariant

$$I = r_{j+1} - r_{j-1}(s_j + t_j) + r_jr^2_{j-1}. \quad (10)$$

By the basic transfer matrices expressed in equations (4, 5), we find that the invariant always equals 2. And there are also two important equalities for $j \geq 2$, which are

$$s_j = t_j,$$
$$s_j + t_j = 2r_{j-1}(r_j - 1). \quad (11)$$

Using equations (10, 11), we attest that the complicated trace map equation (9) can be simplified to

$$r_{j+1} = r^2_{j-1}(r_j - 2) + 2. \quad (12)$$

As usual, defining $\chi_j = \frac{1}{2}\mathrm{Tr}M_j = \frac{1}{2}r_j$, equation (12) can be rewritten into the accustomed form

$$\chi_{j+1} = 4\chi^2_{j-1}(\chi_j - 1) + 1, \quad (13)$$

where $j \geq 2$. It is a striking result and shows that even in a relatively general model of TM dielectric superlattices the trace map takes a form as same as that in the conventional on-site model [17].

Under Born-von Kármán boundary conditions, *i.e.*, $g_{N+1} = g_1$ and $h_{N+1} = h_1$ in equation (6), and at the same time considering the unimodularity of the global transfer matrices, the eigenfrequencies of interface optical modes in the given lth generation of a TM superlattice can be calculated by the equation

$$\chi_l = 1. \quad (14)$$

Combining it with equation (13), we can find two unambiguous facts: Firstly, the solutions of equation (14) are just the roots of following equations

$$\chi_{l-2} = \chi_{l-3} = \cdots = \chi_1 = 0, \quad (15)$$

and

$$\chi_2 = 1. \quad (16)$$

Secondly, the eigenfrequencies of a lower generation of a TM superlattice are preserved in higher generations. The reason is that $\chi_j = 1$ results in

$$\chi_{j+1} = \chi_{j+2} = \cdots = 1, \quad (17)$$

where j is an arbitrary generation number. As shown in the following section, these two facts play central roles in our theoretical analyses of the calculated results.

Each eigenfrequency can create a special distribution of electrostatic potential. First consider the potential amplitudes in A layers. By equations (3, 4), g_m and h_m of the mth block can be obtained iteratively when g_1 and h_1 are given. After g_m and h_m are obtained, the potential amplitude in each A layer can be determined; then the potential distribution in each B layer, characterized by p_m and q_m, can also be calculated through the interface continuum conditions. For a simplified description here, we are only concerned about the averaged potential over each layer. Thus in the mth block we have

$$\phi^A_m = \frac{\sinh(kd^A_m/2)}{kd^A_m/2}(g_m + h_m) \quad (18)$$

for the A layer and

$$\phi_m^B = \frac{1}{kd_m^B}\left\{\left[\sinh kd_m^B + \frac{\varepsilon_A}{\varepsilon_B}(\cosh kd_m^B - 1)\right] g_m \mathrm{e}^{kd_m^A/2} + \left[\sinh kd_m^B - \frac{\varepsilon_A}{\varepsilon_B}(\cosh kd_m^B - 1)\right] h_m \mathrm{e}^{-kd_m^A/2}\right\} \tag{19}$$

for the B layer, where $d_m^A = d_{L(S)}^A$ and $d_m^B = d_{L(S)}^B$ for the mth block being $L(S)$ type.

3 Results and analyses

To get the concrete numerical results of the TM dielectric superlattices studied in this paper, we choose $\varepsilon_{A,\infty} = 2.25$, $\omega_{A,TO} = 31$ THz, and $\omega_{A,LO} = 50$ THz as the values of NaCl; and $\varepsilon_{B,\infty} = 2.1$, $\omega_{B,TO} = 27$ THz, and $\omega_{B,LO} = 40$ THz as the values of KCl.

3.1 Frequency spectra

Figure 1 is the frequency spectrum of coupled optical interface modes of the eighth generation of a TM dielectric superlattice. It can be seen from the spectrum that the allowed frequencies first form four branches, of which two locate between $\omega_{B,TO}$ and $\omega_{A,TO}$ and the other two locate between $\omega_{B,LO}$ and $\omega_{A,LO}$. For the given lth generation of the TM superlattice the frequency number of every branch is $2^{l-1}+2$ and here l equals eight. Our detailed investigation shows that every branch breaks up into six subbands. The first (sixth) and third (fourth) subbands are formed by SS (LL) clusters and other subbands are formed by isolated S (L) blocks. Each subband has almost the same number of modes and splits further. Just as shown in the insets of Figure 1, the second and the fifth subbands are trifurcate (see the right-bottom inset) and the others are bifurcate (see the left-top inset), respectively. All of these are consistent with the branching rules of the electronic energy spectrum of a TM chain in the on-site model [3]. However, the branching rules shown here are different from those of the spectrum of coupled interface optical modes in a Fibonacci dielectric superlattice, where only trifurcation is discovered [10]. This result is not surprising because the branching rules derived from the trace maps depend on the substitution rules.

By the definitions of the basic transfer matrices in equation (4), a quantitative interpretation can be given as to why the frequency spectrum firstly splits into four branches. For convenience, we use a, b, c, and d to denote these four branches. Thus for every frequency ω_a in branch a, there are three corresponding frequencies ω_b, ω_c, and ω_d, which locate respectively in the other three branches b, c, and d. These four frequencies satisfy a relation as

$$\frac{\varepsilon_A(\omega_a)}{\varepsilon_B(\omega_a)} = \frac{\varepsilon_B(\omega_b)}{\varepsilon_A(\omega_b)} = \frac{\varepsilon_B(\omega_c)}{\varepsilon_A(\omega_c)} = \frac{\varepsilon_A(\omega_d)}{\varepsilon_B(\omega_d)}. \tag{20}$$

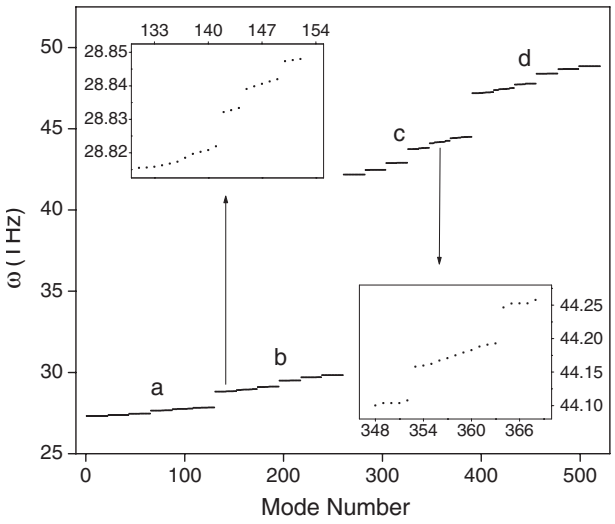

Fig. 1. The frequency spectrum of a TM dielectric superlattice at the eighth generation, where $kd_S^A = 0.5$, $kd_L^A = 1.0$, $kd_S^B = 1.5$, and $kd_L^B = 2.0$. Four branches a, b, c, and d are marked. Inset at top-left: the enlarged pattern of the first subband of branch b, showing bifurcation. Inset at bottom-right: the enlarged pattern of the fifth subband of branch c, showing trifurcation.

Thus one can prove analytically that

$$\chi_j(\omega_a) = \chi_j(\omega_b) = \chi_j(\omega_c) = \chi_j(\omega_d). \tag{21}$$

A simple derivation shows these two relations originate from the factors $(\frac{\varepsilon_B}{\varepsilon_A} + \frac{\varepsilon_A}{\varepsilon_B})$ and $(\frac{\varepsilon_B}{\varepsilon_A} - \frac{\varepsilon_A}{\varepsilon_B})$ in equation (5). Defining $f_1(\varepsilon_A, \varepsilon_B) = \frac{\varepsilon_B}{\varepsilon_A} + \frac{\varepsilon_A}{\varepsilon_B}$ and $f_2(\varepsilon_A, \varepsilon_B) = \frac{\varepsilon_B}{\varepsilon_A} - \frac{\varepsilon_A}{\varepsilon_B}$, one can prove easily that $f_1(\varepsilon_A, \varepsilon_B) = f_1(\varepsilon_B, \varepsilon_A)$ and $f_2(\varepsilon_A, \varepsilon_B) = -f_2(\varepsilon_B, \varepsilon_A)$. Thus we have $\alpha(\varepsilon_A, \varepsilon_B) = \alpha(\varepsilon_B, \varepsilon_A)$, $\beta(\varepsilon_A, \varepsilon_B) = -\beta(\varepsilon_B, \varepsilon_A)$, and $\gamma(\varepsilon_A, \varepsilon_B) = \gamma(\varepsilon_B, \varepsilon_A)$ in equation (5). Interestingly, these transformations of α, β, and γ do not affect the traces of the four basic transfer matrices as well as M_j. Further analyses show that an equation $\frac{\varepsilon_A}{\varepsilon_B} = t$ determines two frequencies ω_a and ω_d, and another equation $\frac{\varepsilon_A}{\varepsilon_B} = \frac{1}{t}$ determines other two frequencies ω_b and ω_c, where t is the solution of equation (14) that locates between -1 and 0. Obviously the four frequencies ω_a, ω_b, ω_c, and ω_d satisfy equations (20, 21).

In fact, this kind of symmetric property of the spectra can now be proved to exist widely in problems of coupled optical interface modes in deterministic aperiodic structures [10,17]. Considering there are four main branches here, we name the property as *quartet* and its effects on the amplitude profiles of electrostatic potentials will be shown in the next subsection.

3.2 Electrostatic potential distributions

The characteristics of the frequency spectra arising from the deterministic aperiodic structure should also be reflected in the distributions of electrostatic potentials,

which are related to the long-wavelength optical vibrations. Actually, the potential distributions are important in Raman scattering [18]. In Figure 2 two amplitude profiles of potential distributions are given. They all have *delocalized* features. To prove analytically that all the potential profiles are *extended* for the lth generation of the TM superlattice, we invoke three Pauli matrices σ_x, σ_y, σ_z, and a 2×2 identity matrix σ_I to resolve the matrices M_j, $\overline{M}_j$, N_j, and $\overline{N}_j$ [6,19], where j is an arbitrary generation number less than or equal to l. After much algebra, one can attest that the eigenfrequencies from the equation $\chi_{j-2} = 0$ strictly render $M_j = \overline{M}_j = \sigma_I$. Combining this result with equation (7), it is easy to make clear that the global transfer matrix for a higher generation ($\geq j$) of the TM superlattice is a periodiclike $N_j\overline{N}_j$ array mixed with the identity matrix σ_I. For example, $M_{j+1} = N_j\overline{N}_j$, $M_{j+2} = \sigma_I N_j \sigma_I \overline{N}_j$, and $M_{j+3} = N_j\overline{N}_j\sigma_I N_j\overline{N}_j N_j\sigma_I\overline{N}_j$, etc. In this way the aperiodic TM superlattice turns into a periodic one by neglecting the layers giving the identity matrix. Thus all the electrostatic potential distributions for the frequencies given by equation (15) are extended. With extended, we mean that amplitudes do not localize in only some layers but spreads through the whole superlattice in a regular way. Besides being extended, they have another interesting feature that the envelope of any amplitude array forms a TM arrangement. Our further analyses show that this property originates from the fact that when $\chi_{j-2} = 0$ the fourth matrix elements of N_j and $\overline{N}_j$ equal zero, which leads to $\phi_j = \phi_{2^j+1} = \phi_{2\times 2^j+1} = \phi_{3\times 2^j+1} = \cdots$. These relations are proved thoroughly by our numerical calculations and can also be discerned from Figure 2, where $j = 3$ and $l = 8$. Clearly the envelope of potential amplitudes forms the fifth generation of the TM sequence.

On the other hand, except the above eigenfrequencies that support delocalized amplitude profiles of electrostatic potentials, the remnants determined by equation (16) do not render M_j and $\overline{M}_j$ being unit matrices and they actually correspond to the potential profiles with linearly growing amplitudes as the layer number of the superlattice increases [19]. Although equation (16) is a polynomial equation of ω with the order being thirty-two, the number of eigenfrequencies determined by this equation is only sixteen because ω must be positive. The numerical calculations further show that these sixteen eigenfrequencies just locate at the band edges of the frequency spectrum shown in Figure 1.

About the electrostatic potential distributions there is another interesting property also named *quartet*, which means that potential profiles given by the four corresponding frequencies determined by equation (20) are exactly the same or very similar. This can be seen from Figure 2. The eigenfrequency for Figure 2a is $\omega_a = 27.755\,114\,128\,271\,59$ THz, which is the 98th mode in Figure 1, and the frequency for Figure 2b is $\omega_b = 28.945\,186\,759\,191\,19$ THz, with the mode number 163. If counted from the upper part of the b branch, the mode number of ω_b is also 98. We confirm that these two frequencies ω_a and ω_b truly satisfy equation (20).

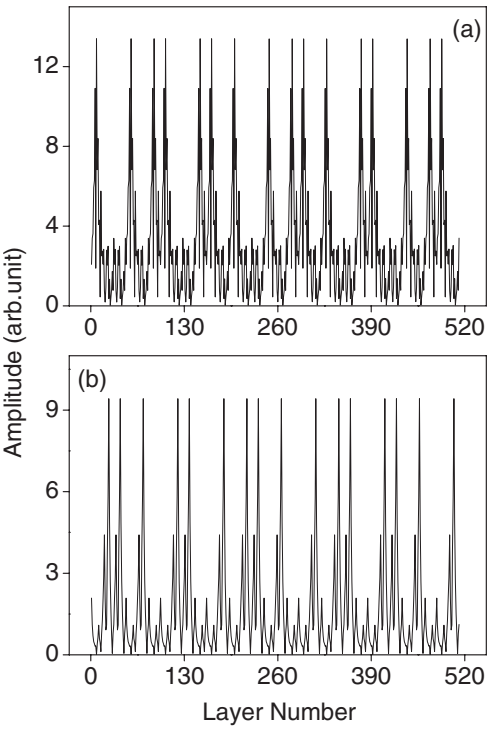

Fig. 2. The *extended* electrostatic potential profiles of four corresponding eigenfrequencies, exhibiting the quartet property. (a) $\omega = 27.755\,114\,128\,271\,59$ THz or $47.441\,231\,630\,188\,96$ THz; (b) $\omega = 28.945\,186\,759\,191\,19$ THz or $44.174\,855\,574\,875\,30$ THz.

By equation (20) we can also work out other two corresponding frequencies ω_c and ω_d, with values as $44.174\,855\,574\,875\,30$ THz and $47.441\,231\,630\,188\,96$ THz and mode numbers as 358 and 423, respectively. The quartet of these four frequencies can be expressed by a numerical relation $98 + 423 = 163 + 358 = 521 = 4 \times (2^{l-1} + 2) + 1$, where $l = 8$. Both electrostatic potential profiles determined by ω_a and ω_d are identical, as shown in Figure 2a; so are other two profiles with ω_b and ω_c, as shown in Figure 2b. The potential profiles given by $\omega_{a(d)}$ and $\omega_{b(c)}$ are not completely the same but they are very similar, and the main modification is that the type of the electrostatic potential distribution changes from $LSSLSLLSSLLSLSSL\cdots$ into $SLLSLSSLLSSLSLLS\cdots$. The cause is that when $\omega_{a(d)} \to \omega_{b(c)}$ the basic transfer matrices undergo $M_{LL} \to M_{LL}^T$ and $M_{SS} \to M_{SS}^T$, where T denotes the transpose of matrices, but $M_{SL} \to M_{SL}^*$ and $M_{LS} \to M_{LS}^*$, where the symbol $*$ represents the following operation of matrices: the second and the third matrix elements multiply negative one and the first and the fourth elements hold the line. Although the basic transfer matrices transform as above, the arranging rule of the matrices does not vary, *i.e.*, the underlying structure feature, which originates from the TM sequence, is still preserved. Thus the *quartet* among the four corresponding potential profiles appears.

4 Summary

We have investigated the properties of coupled optical interface modes in TM dielectric superlattices. The eigenmodes have been calculated in the electrostatic limit by transfer matrices. It has been found that a frequency spectrum first splits into four branches, which indicates the speciality of long wavelength optical phonons in TM superlattices. Except for this point, the branching rules of every branch are completely the same as those of the spectra of other excitations in TM structures [3,11,12], but they are apparently different from the branching rules in periodic and quasiperiodic Fibonacci structures [8,10]. We have also proved rigorously that, except for the potential profiles given by the sixteen frequencies locating at the band edges, the electrostatic potential distributions of TM dielectric superlattices are *extended*. It indicates the TM structure is a distinctive aperiodic structure that lacks translational invariance but supports extended states, which is profoundly different from the Fibonacci structures, where only *critical* eigenstates exist. By critical, we here mean that the eigenstates are neither extended nor localized, but belong to a rigorous singular continuous spectrum. Furthermore, the *quartet* of frequency spectra and electrostatic potential profiles is elucidated analytically and it exhibits the unique property of coupled optical interface modes in TM dielectric superlattices. Lastly, it should be emphasized that dielectric superlattices can be fabricated nicely with current technology, so experimental observation may be fulfilled much conveniently, such as by Raman light scattering, X-ray diffraction measurement, and electron energy-loss spectra, etc. Thus the features of elementary excitations in TM structures will be illustrated.

This work was supported by the Provincial Natural Science Foundation of Jiangsu BK2002086 and the State Key Program for Basic Research of China 001CB610602.

References

1. D. Shechtman, I. Blech, D. Gratias, J.W. Cahn, Phys. Rev. Lett. **53**, 1951 (1984); D. Levine, P.J. Steinhardt, Phys. Rev. Lett. **53**, 2477 (1984)
2. F. Axel, J. Peyriere, J. Stat. Phys. **57**, 1013 (1989)
3. C.S. Ryu, G.Y. Oh, M.H. Lee, Phys. Rev. B **46**, 5162 (1992); **48**, 132 (1993)
4. Nian-hua Liu, Phys. Rev. B **55**, 3543 (1997); Peiqing Tong, Phys. Lett. A **228**, 195 (1997); M.A. Zaks, A.S. Pikovsky, J. Kurths, J. Phys. A **32**, 1523 (1999); S. Chattopadhyay, A. Chakrabarti, J. Phys. Cond. Matt. **12**, 5681 (2000); S. Chattopadhyay, A. Ghosh, A. Chakrabarti, Phys. Rev. B **63**, 064201 (2001)
5. Z. Cheng, R. Savit, R. Merlin, Phys. Rev. B **37**, 4375 (1988); M. Kolar, B. Iochum, L. Raymond, J. Phys. A **26**, 7343 (1993)
6. A. Gosh, S.N. Karmakar, Phys. Rev. B **58**, 2586 (1998); **61**, 1051 (2000)
7. S.F. Cheng, G.J. Jin, Phys. Rev. B **65**, 134206 (2002)
8. R.E. Camly, D. Mills, Phys. Rev. B **29**, 1695 (1984); B.L. Johnson, R.E. Camly, Phys. Rev. B **38**, 3311 (1988)
9. S. Tamura, J.P. Wolfe, Phys. Rev. B **38**, 5610 (1988)
10. G.J. Jin, S.S. Kang, Z. D. Wang, A. Hu, S.S. Jiang, Phys. Rev. B **54**, 11883 (1996)
11. S. Tammura, F. Nori, Phys. Rev. B **40**, 9790 (1989)
12. M.S. Vasconcelos, E.L. Albuquerque, Phys. Rev. B **57**, 2826 (1998)
13. K. Huang, B. Zhu, Phys. Rev. B **38**, 13377 (1988)
14. M. Born, K. Huang, *Dynamical Theory of Crystal Lattice* (Oxford, Clarendon, 1954)
15. A.K. Sood, J. Menéndez, M. Cardona, K. Ploog, Phys. Rev. Lett. **54**, 2115 (1985)
16. M. Kolar, F. Nori, Phys. Rev. B **42**, 1062 (1990)
17. S.F. Cheng, G.J. Jin, R.W. Peng, A. Hu, J. Phys. Soc. Jpn **70**, 2961 (2001)
18. P. Hawrylak, J.J. Quinn, Phys. Rev. Lett. **57**, 380 (1986)
19. A. Chakrabarti, S.N. Karmakar, R.K. Moitra, Phys. Rev. Lett. **74**, 1403 (1995)